

Original Article



Clinical effect of external ventricular drainage under intracranial pressure monitoring in the treatment of aneurysmal subarachnoid hemorrhage patients and investigation of the mechanism of miR-146a-5p/STC1 axis in inhibiting early brain injury in aneurysmal subarachnoid hemorrhage

Changqiang Wang^{1, #}, Jingjing Sun^{2, #}, Junling Liu^{2, *}¹ Department of Intensive Care Unit, Tianjin Huanhu Hospital, Tianjin 300350, China² Department of Intensive Care Unit, Tianjin Fourth Central Hospital, Tianjin 300142, China

Article Info

Abstract



Article history:

Received: January 21, 2024

Accepted: April 23, 2024

Published: May 31, 2024

Use your device to scan and read the article online



Aneurysmal subarachnoid hemorrhage (aSAH) is a common disease in the neural system, with high death rate. Our study aimed to explore the clinical effect of external ventricular drainage under intracranial pressure monitoring in the treatment of patients with aSAH and investigate the role along with mechanism of miR-146a-5p in aSAH. Ninety-six aSAH patients were allocated into control group (CG) and study group (SG). The CG was released by lumbar puncture. The SG underwent external ventricular drainage based on intracranial pressure monitoring. The prognosis, daily living ability, neurological function, S100 β and NSE (neuron-specific enolase) levels and incidence of complications were monitored. Besides, a rat model of SAH was built to assess the neurobehavioral function, blood-brain barrier permeability, brain water content, neuronal apoptosis as well as inflammation. SAH cell model stimulated by oxyhemoglobin, and cell apoptosis as well as inflammation were measured. Luciferase reporter assay was implemented to explore the interaction between miR-146a-5p and STC1. Results showed higher GOS and BI scores but lower NIHSS scores, S100 β and NSE levels and complication rates in SG compared with CG. Additionally, miR-146a-5p presented down-regulation in brain tissues of SAH rat model, and overexpressed miR-146a-5p reduced brain injury along with neuroinflammation in SAH rat model. Oxyhemoglobin-induced nerve cell apoptosis along with inflammation after SAH, and overexpressed miR-146a-5p repressed oxyhemoglobin-induced nerve cell apoptosis along with inflammation. STC1 is the target mRNA of miR-146a-5p, and overexpressed miR-146a-5p represses oxyhemoglobin-induced nerve cell apoptosis along with inflammation via regulating STC1 expression. In conclusion, external ventricular drainage under intracranial pressure monitoring could promote prognosis, promote daily living ability, improve neurological function, reduce S100 β protein and NSE levels, and reduce the incidence of complications in patients with aSAH. Meanwhile, miR-146a-5p inhibited early brain injury and neuroinflammation in aSAH via regulating STC1 expression.

Keywords: Aneurysmal subarachnoid hemorrhage, Early brain injury, External ventricular drainage, Intracranial pressure monitoring, MiR-146a-5p, STC1

1. Introduction

Aneurysmal subarachnoid hemorrhage (aSAH) is mainly caused by aneurysmal hemorrhage (aneurysmal subarachnoid hemorrhage), often accompanied by nausea, vomiting, meningeal irritation, and severe headaches [1]. About 1/4 of patients with aSAH will have hallucinations, delirium, epilepsy, mild hemiplegia, sensory disorders, etc., in severe cases, cerebral vasospasm, hydrocephalus, rebleeding, convulsions, etc [2]. Therefore, the main objective of clinical treatment of aSAH is to prevent complications and reduce the disability rate and fatality rate.

At present, lumbar puncture release of cerebrospinal fluid is commonly applied in clinical therapy of aSAH. Although it can promote the dilution and release of cere-

brospinal bloody fluid to a certain extent, the overall treatment effect is poor and the prognosis of most patients is poor due to the difficulty in mastering the drainage flow of cerebrospinal fluid and the need for repeated lumbar puncture [3]. Recently, with the continuous development and improvement of medical technology, external ventricular drainage under intracranial pressure monitoring has been recognized by clinicians and patients because it has fewer complications and is beneficial to promote the quality of life of aSAH patients [4], but there are few reports on its application effect in patients with aSAH.

SAH is also associated with a variety of complications that can lead to early brain injury (EBI). EBI means direct brain injury along with secondary pathophysiological reac-

* Corresponding author.

E-mail address: tjsjjss5698@163.com (J. Liu).

These authors contributed equally

Doi: <http://dx.doi.org/10.14715/cmb/2024.70.5.44>

tions in 72 h after aSAH, containing elevated intracranial pressure as well as reduced cerebral blood flow, leading to cerebral ischemia [5]. These alterations immediately result in neuronal death, changes in blood-brain barrier (BBB) permeability, along with brain edema. Although efforts have been made in SAH treatment, which has improved the survival rate of patients by 17%, most patients still have varying degrees of neurological and cognitive dysfunction [6]. Hence, a deeper comprehension of the potential molecular mechanisms associated with EBI paves the way for novel prevention methods as well as treatments that may lead to EBI after aSAH.

MicroRNAs (miRNAs) belong to widespread RNA molecules of approximately 21-23 nucleotides in eukaryotes, which represses the translation of mRNA via combining with the 3'-untranslated region (UTR) of the target mRNA [7]. As reported previously, miRNAs are crucial modulators in various neurological diseases. For example, miR-9-5p represses the MMP⁺-stimulated neuron apoptosis in Parkinson's disease through SCRIB/ β -Catenin signaling [8]. MiR-144 promotes microglial autophagy as well as inflammation after intracerebral hemorrhage [9]. Besides, many miRNAs containing miR-706 as well as miR-130b are also discovered to be dysregulated during aSAH pathogenesis [10]. Of note, miR-146a-5p has been documented to be low-expressed in aSAH patients, but its function in aSAH has not been investigated.

In our research, we aimed to explore the clinical impact of external ventricular drainage under intracranial pressure monitoring in the treatment of patients with aSAH and investigate the role along with mechanism of miR-146a-5p in aSAH.

2. Material and methods

2.1. Patient data

Ninety-six aSAH patients who received therapy in our hospital from March 2021 to June 2023 were chosen, followed by dividing into control group (CG) and study group (SG) according to cerebrospinal fluid drainage methods, with 48 cases in each group. The CG contained 28 males together with 20 females. The average age was (45.62±15.42) years, ranging 19-73 years; Subarachnoid hemorrhage Hunt&Hess classification: grade II (17 cases), grade III (18 cases), grade IV (10 cases), grade V (3 cases); Aneurysm location: 6 cases of anterior cerebral artery A1 segment, 14 cases of posterior communicating artery, 28 cases of anterior communicating artery. The SG contained 27 males together with 21 females. The average age was (45.65±15.45) years, ranging 20-74 years; Subarachnoid hemorrhage Hunt&Hess classification: grade II (16 cases), grade III (19 cases), grade IV (11 cases), grade V (2 cases); Aneurysm location: 7 cases of anterior cerebral artery A1 segment, 15 cases of posterior communicating artery, 26 cases of anterior communicating artery. No difference was discovered in general data between 2 groups ($P>0.05$).

Inclusion criteria: (1) Subarachnoid hemorrhage was confirmed by craniocerebral CT examination and aneurysm was confirmed by craniocerebral CT angiography (CTA) examination; (2) Hospital admission within 24 hours of onset; (3) Patients gave informed consent to the study. Exclusion criteria: (1) Patients with coagulopathy; (2) Patients with severe liver, kidney along with other important organ dysfunction; (3) Patients with traumatic subarachnoid hemorrhage; (4) Patients with other types of

spontaneous subarachnoid hemorrhage; (5) Hydrocephalus, cerebrovascular spasm and other complications.

2.2. Treatment methods

After admission, patients in 2 groups adopted routine symptomatic treatment containing controlling blood pressure, reducing intracranial pressure, oxygen inhalation, improving microcirculation, anti-inflammatory, correcting water and electrolyte disorders, mild hypothermia therapy, and nutritional cranial nerve.

Patients in the CG were released by lumbar puncture on the basis of conventional symptomatic treatment: lumbar puncture was performed to release cerebrospinal fluid on the second day after admission, once a day, for 8-10 days, cerebrospinal fluid biochemistry and routine examination of cerebrospinal fluid were performed every day until the protein content of cerebrospinal fluid was <0.4 g/L and the red blood cell count was reduced to $<100\times 10^6$ /L. After puncture, the cerebrospinal fluid was replaced with 0.9% sodium chloride solution.

Patients in the SG underwent external ventricular drainage based on intracranial pressure monitoring on the basis of conventional symptomatic treatment: after clipping the aneurysm, the subarachnoid space was cleaned, intracranial pressure was monitored with an intraventricular intracranial pressure probe once/h, and external ventricular drainage was performed with the frontal Angle as the puncture point. Nimodipine was given to patients with intracranial pressure greater than 25 mm Hg (1 mm Hg=0.133 kPa) to maintain intracranial pressure within the reference range.

Dynamic craniocerebral CT examination was performed in both groups.

2.3. Observation indicators

Glasgow Prognostic Scale (GOS) was used to evaluate the prognosis 6 months after surgery [11]. The total score was 1-5, with 1 being death. The higher score indicated better prognosis.

Barthel index (BI) was adopted to evaluate the daily living ability of 2 groups before and 6 months after surgery [12], with the total score ranging 0-100. The higher score represented better daily living ability.

National Institutes of Health Stroke Scale (NIHSS) was implemented to evaluate the neurological defects of 2 groups before and 6 months after surgery [13]. The lower the score, the better the neurological function was.

3 mL of fasting venous blood was gathered before as well as 6 months after surgery, and serum was acquired after centrifugation. S100 β protein and (neuron-specific enolase) NSE levels were determined by enzyme-linked immunosorbent assay.

The incidence of complications, including infection, cerebral infarction, epilepsy, and hydrocephalus were compared between 2 groups during hospitalization.

2.4. SAH model in rats

Adult male Sprague-Dawley (SD) rats, weighing 230 ~ 335 g, were placed in a specific pathogen-free animal laboratory with constant temperature and humidity, free access to food and water, and a light and dark cycle of 12 h/12 h. This experiment was approved by the Animal Ethics Committee of the hospital.

The rat SAH model was established using the method

described in the literature. The operation was as follows: the rats were anesthetized with 3% isoflurane and subjected to mechanical ventilation. A sharp 4-0 monofilament nylon suture was inserted from the external carotid artery into the internal carotid artery. Then a further 3 mm was advanced to puncture the blood vessel, the nylon sutures were pulled out, the external carotid artery was lapped to restore blood flow, and the wound was stitched to allow the rat to recover on a heated blanket. After 1 h of SAH modeling, SAH-stimulated rats received injections with miR-146a-5p agomir and agomir NC in stereotaxic ventricle. Healthy rats underwent the same operation without perforating the blood vessels and were set as the sham group.

2.5. Stereotaxic lateral ventricular injection

MiR-146a-5p agomir and agomir NC were purchased from Shanghai GenePharma (Shanghai, China). One hour following SAH model was established, 2.5% isoflurane-anesthetized rats were fixed on Stoelting animal stereotaxic apparatus. Afterwards, MiR-146a-5p agomir or agomir NC (0.5 μ L/min) was injected with a 10 μ L syringe at 3.5 mm submeningeal, 1.5 mm outside the right ventricle (right), and 0.9 mm posterior to the right ventricle, using the fontanel as a reference point. Next, the needle was slowly pulled out, the pores were sealed with bone wax, the scalp was sutured, and an electric blanket was used to keep warm before anesthesia.

2.6. Neurobehavioral tests

Neurobehavioral tests were performed 24 h after SAH and evaluated via an improved Garcia score method [14]. The neurobehavioral test was administered by 2 independent researchers, and average scores were calculated.

2.7. Morphological observation of rat brain

The rats were sacrificed, and the brain tissue could be isolated, dehydrated, embedded, followed by cutting into 5 μ m slices, and HE staining was implemented to observe the histopathology and pathology of rat brain under microscope.

2.8. Cerebral water content determination

The brain tissues of the rats were gathered immediately after euthanasia, followed by separating into right hemisphere, left hemisphere, cerebellum, as well as brainstem. They weigh the above parts (recorded to be wet weight) and place them in an oven at 105°C for 3 consecutive days. Then weigh the dry brain, called dry weight; Brain water content = [(wet weight - dry weight)/(wet weight)] \times 100%.

2.9. Blood-brain barrier (BBB) test

The BBB permeability was assessed by Evans Blue exudation. Evans Blue dye (2%, 5 mL/kg) was injected through the right femoral vein, and normal saline was injected through the cardiac vein until the drainage was colorless. Afterwards, the brain tissue was separated, milled, and centrifuged, followed by obtaining the supernatant. The same amount of ethanol trichloroacetic acid was added to the sample for incubation at 4°C overnight. The absorbance of the sample could be measured by UV-VIS spectrophotometer at 620 nm. The EB solution standard curve was drawn with 50 ~ 1000 ng/mL Ethidium bromide (EB) standard solution. The absorbance value of the sample was compared with the EB standard curve to cal-

culate the EB level of the sample.

2.10. RT-qPCR

Total RNA was extracted from harvested cortex tissues by help of RNAiso Plus (Takara Bio, Dalian, China). PrimeScript RT Master Mix (Takara, Japan) was implemented for the reverse transcription of RNA to cDNA. RT-qPCR was implemented using Hieff® qPCR SYBR Green Master Mix (Yeasen, China). The 2^{- $\Delta\Delta$ Ct} method was adopted to identify the gene relative expression levels.

2.11. TUNEL

The rat brain tissue was fixed, dehydrated, and impregnated with wax for embedding. The tissues were sliced 4 m thick, roasted at 60°C for 3 h, and dewaxed. According to the Apo Alert TUNEL cell apoptosis detection kit instructions (Biosciences Clontech, USA), the sections were finally sealed with a sealing solution including anti-fluorescence quencher, and the images could be observed via a fluorescence microscope to calculate the proportion of apoptotic nerve cells.

2.12. ELISA

The brain tissue samples were ground and placed in a centrifuge tube, homogenized in the bath with a high-speed homogenizer, centrifuged, and the supernatant was extracted following the kit instructions. ELISA was adopted to detect the concentrations of IL-6, IL-1 β as well as TNF- α .

2.13. Cell culture and in vitro SAH model

Murine HT22 cells were cultivated in Dulbecco's modified Eagle medium (DMEM) which contained 10% fetal bovine serum along with 1% penicillin/streptomycin at 37°C with CO₂. Oxyhemoglobin (5 μ M) was added into the culture medium for 24 h to stimulate SAH damage in vitro.

2.14. Cell transfection

MiR-146a-5p mimics and NC mimics, along with pcDNA3.1-STC1 and pcDNA3.1 were purchased from GenePharma (Shanghai, China). Cell transfection was implemented using Lipofectamine 2000 (Thermo Fisher, USA).

2.15. CCK-8

Cells were planted in 96-well plates, and then CCK-8 reagent (10 μ L) mixed with 90 μ L of complete medium was added to each well for 1.5 h of cultivation. The optical density was tested at 450 nm by means of a microplate reader.

2.16. Flow cytometry

Cells were digested, collected, washed, and resuspended. Then, 5 μ L Annexin V-FITC, as well as 5 μ L Propidium Iodide, were added into cells for reaction in the dark for 15 min at room temperature. Cell apoptosis was analyzed by flow cytometry.

2.17. Luciferase reporter assay

Cells were planted into 12-well plates, followed by co-transfection with luciferase plasmids of STC1 3'UTR-WT/MUT in the pmirGlo vector (GenePharma, China) or miR-146a-5p mimics/NC mimics for 24 h. The Dual-

Luciferase Reporter Assay System (Promega, USA) was implemented to assess the luciferase activity.

2.18. Statistical analysis

Statistical analysis was implemented with Graph-Pad Prism. All experiments were performed more than 3 times. Data that satisfied normality and homogeneity of variance were exhibited as the mean \pm standard deviation (SD) and analyzed with student t-test or one-way analysis of variance (ANOVA) followed by multiple comparisons using Tukey's post hoc analysis. Statistical difference was defined as $P < 0.05$.

3. Results

3.1. Clinical effect of external ventricular drainage under intracranial pressure monitoring in the treatment of patients with aSAH

Six months after surgery, the GOS score of the SG presented higher when compared with the CG ($P < 0.01$, Fig. 1A). Before surgery, no difference was discovered in BI score between 2 groups ($P > 0.05$). Six months after surgery, the BI score was elevated in 2 groups, and that in the SG presented elevation when compared with the CG ($P < 0.05$, Fig. 1B). Before surgery, no difference was discovered in NIHSS score between 2 groups ($P > 0.05$). Six months after surgery, the NIHSS score was lessened in 2 groups, and that in the SG presented lower when compared with the CG ($P < 0.05$, Fig. 1C). Before surgery, no difference was discovered in S100 β and NSE levels between 2 groups ($P > 0.05$). Six months after surgery, the S100 β and NSE levels were lessened in 2 groups, and those in the SG presented reduction when compared with the CG ($P < 0.05$, Fig. 1D-E). Table 1 displayed that the incidence of complications in the SG presented reduction when compared with the CG ($P < 0.05$).

3.2. Overexpressed miR-146a-5p reduces brain injury and neuroinflammation in SAH rat model

In the SAH group, the Garcia score could be decreased, the BBB permeability was increased, and the brain water content was enhanced (Fig. 2A-C). HE staining was used to assess the brain damage in rats. In the sham group, the cortical structure was intact, the neuronal morphology was normal, the nucleus was intact and blue spherical, the cytoplasm was light stained, and there was no neuronal damage. In the SAH group, the cortical structure of rats was disorganized and loose, the number of neurons was lessened, as well as the pathological changes such as nuclear pyretic contraction and deep staining were observed, and the brain tissue and neurons were damaged (Fig. 2D). Subsequently, the cerebral cortex tissue was sliced and TUNEL staining was implemented to detect neuronal apoptosis. The number of TUNEL-positive cells was elevated in the SAH group (Fig. 2E). ELISA unveiled that IL-1 β , IL-6 along with TNF- α levels presented higher in the SAH group (Fig. 2F). In addition, miR-146a-5p presented

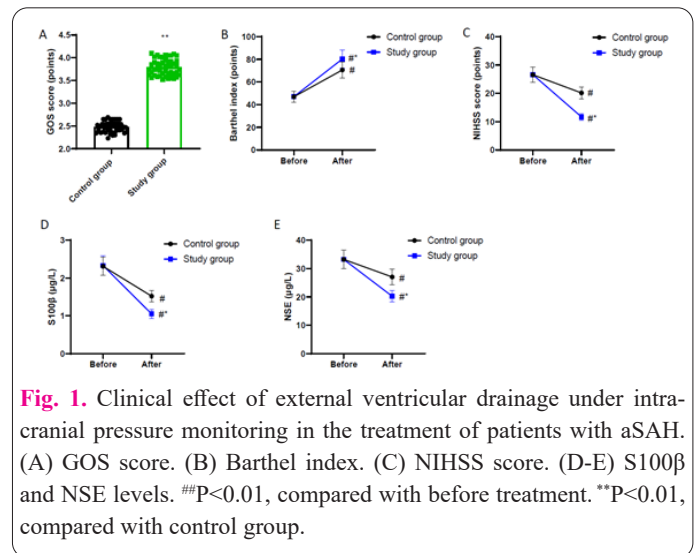


Fig. 1. Clinical effect of external ventricular drainage under intracranial pressure monitoring in the treatment of patients with aSAH. (A) GOS score. (B) Barthel index. (C) NIHSS score. (D-E) S100 β and NSE levels. ## $P < 0.01$, compared with before treatment. ** $P < 0.01$, compared with control group.

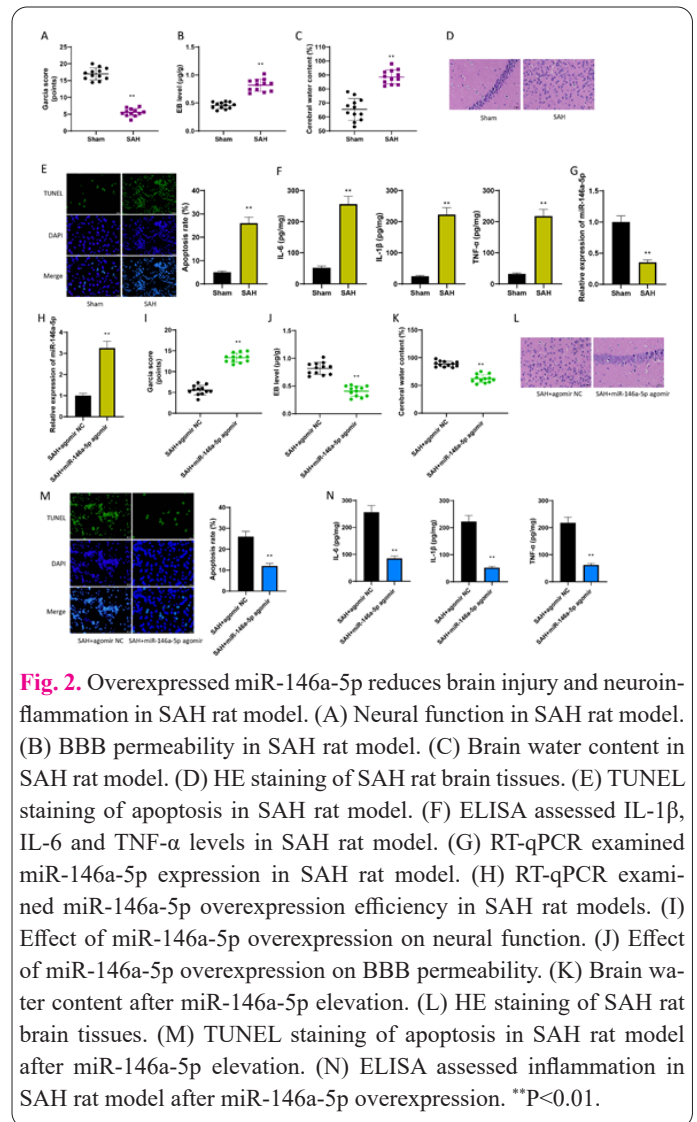


Fig. 2. Overexpressed miR-146a-5p reduces brain injury and neuroinflammation in SAH rat model. (A) Neural function in SAH rat model. (B) BBB permeability in SAH rat model. (C) Brain water content in SAH rat model. (D) HE staining of SAH rat brain tissues. (E) TUNEL staining of apoptosis in SAH rat model. (F) ELISA assessed IL-1 β , IL-6 and TNF- α levels in SAH rat model. (G) RT-qPCR examined miR-146a-5p expression in SAH rat model. (H) RT-qPCR examined miR-146a-5p overexpression efficiency in SAH rat models. (I) Effect of miR-146a-5p overexpression on neural function. (J) Effect of miR-146a-5p overexpression on BBB permeability. (K) Brain water content after miR-146a-5p elevation. (L) HE staining of SAH rat brain tissues. (M) TUNEL staining of apoptosis in SAH rat model after miR-146a-5p elevation. (N) ELISA assessed inflammation in SAH rat model after miR-146a-5p overexpression. ** $P < 0.01$.

down-regulation in the SAH group (Fig. 2G).

First, miR-146a-5p agomir was transfected into the

Table 1. Incidence of complications in 2 groups.

Groups	Cases	Infection	Cerebral infarction	Epilepsy	Hydrocephalus	Total incidence rate
Control	48	4	1	2	2	9 (18.75%)
Study	48	1	0	1	0	2 (4.17%)
χ^2						5.031
P						0.024

brain of SAH rats, in order to elevate miR-146a-5p expression (Fig. 2H). SAH rats transfected with miR-146a-5p agomir unveiled enhanced neural function scores, decreased BBB permeability, and decreased brain water content (Fig. 2I-K). HE staining displayed that the pathological damage of brain tissue and neurons in the miR-146a-5p agomir group could be reduced (Fig. 2L). TUNEL staining showed that the apoptosis rate of neurons in miR-146a-5p agomir group could be significantly reduced (Fig. 2M). ELISA showed that IL-1 β , IL-6 as well as TNF- α levels in miR-146a-5p agomir group were lessened (Fig. 2N).

3.3. Overexpressed miR-146a-5p represses oxyhemoglobin-stimulated nerve cell apoptosis along with inflammation

It was observed in CCK-8 assay that oxyhemoglobin treatment apparently reduced HT22 cells viability (Fig. 3A). Meanwhile, flow cytometry analysis indicated that oxyhemoglobin treatment apparently elevated HT22 cells apoptosis (Fig. 3B). As for inflammation, oxyhemoglobin treatment enhanced IL-1 β , IL-6 along with TNF- α levels in HT22 cells (Fig. 3C). RT-qPCR results displayed that oxyhemoglobin could reduce miR-146a-5p expression in HT22 cells (Fig. 3D). Thus, we elevated miR-146a-5p expression in HT22 cells to assess the impacts of miR-146a-5p overexpression on oxyhemoglobin-stimulated nerve cell apoptosis along with inflammation (Fig. 3E). As displayed in Fig. 3F-H, miR-146a-5p overexpression definitely elevated the viability as well as repressed apoptosis and inflammation in oxyhemoglobin-induced HT22 cells.

3.4. STC1 is the target mRNA of miR-146a-5p

Through microT, RNA22 and Targetscan databases, STC1 was predicted to have binding sites with miR-146a-5p (Fig. 4A), and the binding sites between them were displayed in Fig. 4B. Through luciferase report assay, we proved that the luciferase activity of STC1 3'UTR-WT could be weakened after miR-146a-5p overexpression,

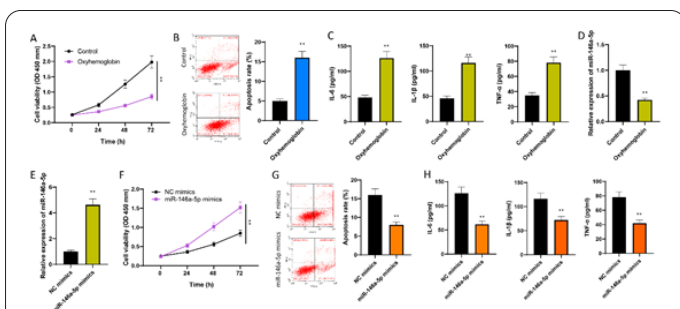


Fig. 3. Overexpressed miR-146a-5p represses oxyhemoglobin-stimulated nerve cell apoptosis along with inflammation. (A) CCK-8 assessed HT22 cell viability after oxyhemoglobin treatment. (B) Flow cytometry analysis assessed HT22 cells apoptosis after oxyhemoglobin treatment. (C) ELISA examined inflammation in HT22 cells apoptosis after oxyhemoglobin treatment. (D) RT-qPCR detected miR-146a-5p expression in oxyhemoglobin-treated HT22 cells. (E) RT-qPCR examined miR-146a-5p overexpression efficiency in oxyhemoglobin-treated HT22 cells. (F) CCK-8 assessed oxyhemoglobin-treated HT22 cell viability after miR-146a-5p overexpression. (G) Flow cytometry analysis assessed oxyhemoglobin-treated HT22 cell apoptosis after miR-146a-5p elevation. (H) ELISA examined inflammation in oxyhemoglobin-treated HT22 cells apoptosis after miR-146a-5p elevation. ** $P < 0.01$.

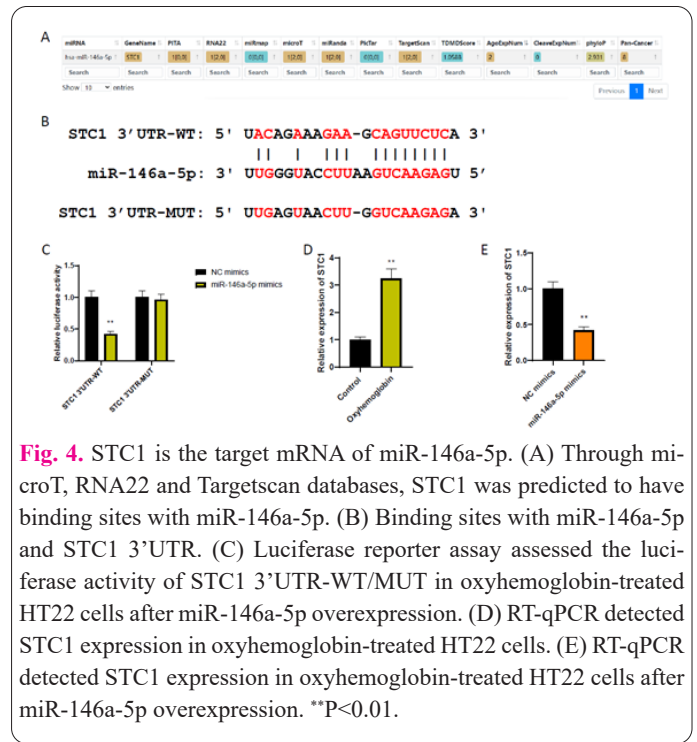


Fig. 4. STC1 is the target mRNA of miR-146a-5p. (A) Through microT, RNA22 and Targetscan databases, STC1 was predicted to have binding sites with miR-146a-5p. (B) Binding sites with miR-146a-5p and STC1 3'UTR. (C) Luciferase reporter assay assessed the luciferase activity of STC1 3'UTR-WT/MUT in oxyhemoglobin-treated HT22 cells after miR-146a-5p overexpression. (D) RT-qPCR detected STC1 expression in oxyhemoglobin-treated HT22 cells. (E) RT-qPCR detected STC1 expression in oxyhemoglobin-treated HT22 cells after miR-146a-5p overexpression. ** $P < 0.01$.

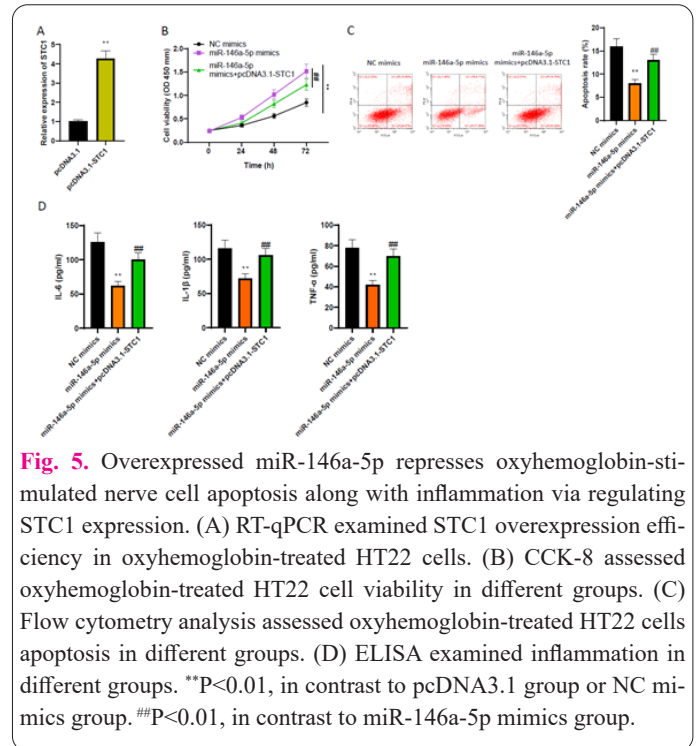


Fig. 5. Overexpressed miR-146a-5p represses oxyhemoglobin-stimulated nerve cell apoptosis along with inflammation via regulating STC1 expression. (A) RT-qPCR examined STC1 overexpression efficiency in oxyhemoglobin-treated HT22 cells. (B) CCK-8 assessed oxyhemoglobin-treated HT22 cell viability in different groups. (C) Flow cytometry analysis assessed oxyhemoglobin-treated HT22 cells apoptosis in different groups. (D) ELISA examined inflammation in different groups. ** $P < 0.01$, in contrast to pcDNA3.1 group or NC mimics group. ## $P < 0.01$, in contrast to miR-146a-5p mimics group.

but the luciferase activity of STC1 3'UTR-MUT was not changed (Fig. 4C). Besides, we discovered that oxyhemoglobin treatment could elevate STC1 expression in HT22 cells (Fig. 4D). More importantly, STC1 expression could be repressed in oxyhemoglobin-treated HT22 cells after miR-146a-5p overexpression (Fig. 4E).

3.5. Overexpressed miR-146a-5p represses oxyhemoglobin-stimulated nerve cell apoptosis along with inflammation via regulating STC1 expression

We elevated STC1 expression in oxyhemoglobin-treated HT22 cells (Fig. 5A), followed by performing rescue assays to certify whether overexpressed miR-146a-5p represses oxyhemoglobin-stimulated nerve cell apoptosis along with inflammation via regulating STC1 expression. It was discovered in Fig. 5B-D that the elevated viability as

well as the lessened apoptosis and inflammation caused by miR-146a-5p elevation in oxyhemoglobin-treated HT22 cells could be offset after co-transfection of pcDNA3.1-STC1.

4. Discussion

The results of epidemiological investigation have shown that the annual prevalence of aSAH is 10.6/100,000, accounting for 22% of all cerebrovascular lesions and 80% of spontaneous subarachnoid hemorrhage [15]. Cerebrovascular malformation, abnormal vascular network disease of skull base, vasculitis, and connective tissue diseases are risk factors for sSAH, while EBI is a risk factor for death of sSAH patients [16]. Subarachnoid hemorrhage can lead to calcium overload and metabolic disorders of cerebral microvascular endothelial cells, and then destroy neuronal skeleton and nuclear contraction, leading to neuronal swelling and even apoptosis [17]. At the same time, blood flow into the subarachnoid space through the ruptured blood vessels can lead to the secretion of vasoconstrictor substances such as prostaglandin, vascular endothelin, catecholamine, and then cause smooth muscle tonic contraction and aggravate cerebral vasospasm [18]. Therefore, early removal of hemorrhagic cerebrospinal fluid is essential in decreasing the incidence of cerebral vasospasm along with improving the prognosis of patients with aSAH.

Release of cerebrospinal fluid by lumbar puncture is a common method to remove the hemorrhagic cerebrospinal fluid, which can improve the circulation of cerebrospinal fluid by reducing the stimulation of hemorrhagic cerebrospinal fluid. However, excessive drainage of cerebrospinal fluid can lead to ventricle shrinkage, brain hernia, brain tissue retraction, etc., resulting in bridge vein rupture and hemorrhage and intracranial hematoma. Recent literatures have shown that the mortality rate of aSAH patients with recurrent aneurysm rupture is about 70%, among which the duration of intracranial hypertension and the degree of intracranial pressure increase are risk factors for the death of aSAH patients with recurrent aneurysm rupture, mainly related to the continuous increase of intracranial pressure leading to consciousness disturbance and brain hernia [19]. Therefore, effectively reducing cerebral edema and improving cerebral perfusion pressure have crucial clinical significance in declining the risk of death in aSAH patients.

External ventricular drainage under intracranial pressure monitoring is a new hemorrhagic cerebrospinal fluid drainage method. Intracranial pressure monitoring is helpful in guiding clinicians to accurately assess the degree of craniocerebral injury and early detection of intracranial space, which is conducive to reducing secondary brain injury and improving the prognosis of patients. The placement of intracranial intraventricular pressure probe is conducive to dynamic monitoring of intracranial pressure changes, effectively avoiding increased blood viscosity, renal function injury, and electrolyte disturbance caused by blind application of dehydrating agents, shortening the placement time of drainage tube and reducing the risk of intracranial infection [20]. Intracranial pressure monitoring can determine the drainage flow according to intracranial pressure, which can effectively avoid rebleeding caused by intracranial pressure fluctuation [21].

In our study, we explored the clinical effect of external

ventricular drainage under intracranial pressure monitoring in the treatment of patients with aSAH, and discovered that in contrast to the CG, the GOS score of the SG presented elevation, the BI score in the SG presented higher, the NIHSS score in the SG presented reduction, and the incidence of complications in the SG presented reduction, suggesting that external ventricular drainage under intracranial pressure monitoring could promote prognosis, promote daily living ability, improve neurological function and repress the incidence of complications of aSAH patients, which was in accordance with previous report [22].

After the occurrence of chronic hydrocephalus after aSAH, the neurons of the body are damaged, and NSE enters the blood through the injured BBB, resulting in the increase of NSE level [23]. S100 β protein is produced by astrocytes and oligodendrocytes. When the BBB is damaged, S100 β protein is released by the injured cells [24]. Our study also indicated that after treatment, the S100 β and NSE levels in the SG presented reduction when compared with the CG, suggesting that external ventricular drainage under intracranial pressure monitoring could improve BBB permeability in patients with aSAH.

Some research has found that miRNA is closely linked to neuropathology and can be used to be a possible biomarker for EBI therapy after SAH [25]. The potential of miR-146a-5p in human malignancies has been extensively studied [26]. Moreover, it has been documented that miR-146a-5p relieves neuropathic pain via repressing TRAF6 signaling in the spinal cord [27]. Notably, this study was the first to study the potential of miR-146a-5p in rat and cellular models of SAH. It was discovered that miR-146a-5p presented down-regulation. The causes of EBI within 72 h after SAH include abnormal cerebral blood flow regulation, disorders of cerebral metabolism, damage to the BBB, inflammatory factors, and thrombosis pathways [28]. Neuronal apoptosis is considered to be the key event of EBI after SAH, and is the cause of neurological injury in SAH patients. In addition, physiological abnormalities during EBI trigger an inflammatory cascade leading to the destruction of the BBB and neuronal degeneration [29]. The expression levels of inflammatory factors containing IL-1 β , IL-6 as well as TNF- α in SAH patients are up-regulated, which can accelerate brain injury by elevating apoptosis pathway [30].

In our study, we established a rat model of SAH as well as SAH cell model induced by oxyhemoglobin and discovered that miR-146a-5p presented down-regulation in brain tissues of SAH rat model and oxyhemoglobin-treated HT22 cells. Besides, our study revealed that overexpressed miR-146a-5p reduced brain injury as well as neuroinflammation in SAH rat model and hindered oxyhemoglobin-induced nerve cell apoptosis along with inflammation, suggesting that miR-146a-5p exerted a protective function in SAH, which was similar to a study proposed by Mai et al. [31].

Stanniocalcin-1 (STC1) belongs to a homodimeric glycoprotein hormone [32] and is expressed in diverse normal organs containing the skin, lung, ovary, along with cervix, [33]. Studies have discovered that STC1 plays a role in neurological diseases, including glioma as well as ischemic stroke [34]. Notably, it has been reported that serum STC1 concentration presents elevation in aSAH patients [35-37]. In our research, we discovered that STC1 was

proved to be the target gene of miR-146a-5p, and further rescue assays indicated that overexpressed miR-146a-5p hindered oxyhemoglobin-stimulated nerve cell apoptosis along with inflammation via regulating STC1 expression.

5. Conclusion

In conclusion, our study demonstrates that external ventricular drainage under intracranial pressure monitoring can promote prognosis, promote daily living ability, improve neurological function, reduce S100 β protein and NSE levels and reduce the incidence of complications of patients with aSAH. Meanwhile, miR-146a-5p inhibits EBI and neuroinflammation in aSAH via regulating STC1 expression.

Conflict of Interests

The authors declare no competing interests.

Consent for publications

The author read and approved the final manuscript for publication.

Ethics approval and consent to participate

We have received approval from the Ethics Committee of Tianjin Huanhu Hospital and Tianjin Fourth Central Hospital.

Informed Consent

We have received informed consent from the Ethics Committee of Tianjin Huanhu Hospital and Tianjin Fourth Central Hospital.

Availability of data and material

If you have any additional questions about the study's original contributions, please contact the corresponding author.

Authors' contributions

LJ contributed to the study conception and design. Experimental operation, data collection and analysis were performed by WC and SJ. The first draft of the manuscript was written by WC. All authors commented on previous versions of the manuscript.

Funding

Not applicable.

Acknowledgement

Not applicable.

References

- Langer T, Zadek F, Carbonara M, Caccioppola A, Brusatori S, Zoerle T, Bottazzini F, Ferraris Fusarini C, di Modugno A, Zannella A, Zanier ER, Fumagalli R, Pesenti A, Stocchetti N (2022) Cerebrospinal Fluid and Arterial Acid-Base Equilibrium of Spontaneously Breathing Patients with Aneurismal Subarachnoid Hemorrhage. *Neurocrit Care* 37 (1): 102-110. doi: 10.1007/s12028-022-01450-1
- Fiorindi A, Vezzoli M, Doglietto F, Zanin L, Saraceno G, Agosti E, Barbieri A, Bellocchi S, Bernucci C, Bongetta D, Cardia A, Costi E, Egidi M, Fioravanti A, Gasparotti R, Giussani C, Grimod G, Latronico N, Locatelli D, Mardighian D, Nodari G, Poli JC, Rasulo F, Roca E, Sicuri GM, Spina G, Stefani R, Vivaldi O, Zoia C, Calza S, Fontanella MM, Cenzato M (2022) Aneurismal subarachnoid hemorrhage during the COVID-19 outbreak in a Hub and Spoke system: observational multicenter cohort study in Lombardy, Italy. *Acta Neurochir (Wien)* 164 (1): 141-150. doi: 10.1007/s00701-021-05013-9
- Petridis AK, Kamp MA, Cornelius JF, Beez T, Beseoglu K, Turrowski B, Steiger HJ (2017) Aneurysmal Subarachnoid Hemorrhage. *Dtsch Arztebl Int* 114 (13): 226-236. doi: 10.3238/arztebl.2017.0226
- Qian C, Yu X, Chen J, Gu C, Wang L, Chen G, Dai Y (2016) Effect of the drainage of cerebrospinal fluid in patients with aneurismal subarachnoid hemorrhage: A meta-analysis. *Medicine (Baltimore)* 95 (41): e5140. doi: 10.1097/md.00000000000005140
- Deng X, Wu Y, Hu Z, Wang S, Zhou S, Zhou C, Gao X, Huang Y (2023) The mechanism of ferroptosis in early brain injury after subarachnoid hemorrhage. *Front Immunol* 14: 1191826. doi: 10.3389/fimmu.2023.1191826
- Pang J, Peng J, Yang P, Kuai L, Chen L, Zhang JH, Jiang Y (2019) White Matter Injury in Early Brain Injury after Subarachnoid Hemorrhage. *Cell Transplant* 28 (1): 26-35. doi: 10.1177/0963689718812054
- Saliminejad K, Khorram Khorshid HR, Soleymani Fard S, Ghafari SH (2019) An overview of microRNAs: Biology, functions, therapeutics, and analysis methods. *J Cell Physiol* 234 (5): 5451-5465. doi: 10.1002/jcp.27486
- Xiao Z, Yan Z, Sun X, Zhu Z, Wang B, Gao M, Lu F, Liu J, Zong Z, Zhang H, Guo Y (2022) MiR-9-5p Inhibits the MMP(+)-Induced Neuron Apoptosis through Regulating SCRIB/ β -Catenin Signaling in Parkinson's Disease. *Oxid Med Cell Longev* 2022: 9173514. doi: 10.1155/2022/9173514
- Yu A, Zhang T, Zhong W, Duan H, Wang S, Ye P, Wang J, Zhong S, Yang Z (2017) miRNA-144 induces microglial autophagy and inflammation following intracerebral hemorrhage. *Immunol Lett* 182: 18-23. doi: 10.1016/j.imlet.2017.01.002
- Huang Z, Hu J, Xu J, Wang H, Dai L (2023) microRNA-130b May Induce Cerebral Vasospasm after Subarachnoid Hemorrhage via Modulating Kruppel-like Factor 4. *Mol Cell Biol* 43 (7): 301-316. doi: 10.1080/10985549.2023.2210030
- Roquilly A, Moyer JD, Huet O, Lasocki S, Cohen B, Dahyot-Fizelier C, Chalard K, Seguin P, Jeantrelle C, Vermeersch V, Gaillard T, Cinotti R, Demeure Dit Latte D, Mahe PJ, Vourc'h M, Martin FP, Chopin A, Lerebourg C, Flet L, Chiffolleau A, Feuillet F, Asehnoune K (2021) Effect of Continuous Infusion of Hypertonic Saline vs Standard Care on 6-Month Neurological Outcomes in Patients With Traumatic Brain Injury: The COBI Randomized Clinical Trial. *JAMA* 325 (20): 2056-2066. doi: 10.1001/jama.2021.5561
- Quinn TJ, Langhorne P, Stott DJ (2011) Barthel index for stroke trials: development, properties, and application. *Stroke* 42 (4): 1146-1151. doi: 10.1161/strokeaha.110.598540
- Kwah LK, Diong J (2014) National Institutes of Health Stroke Scale (NIHSS). *J Physiother* 60 (1): 61. doi: 10.1016/j.jphys.2013.12.012
- Matsumura K, Kumar TP, Guddanti T, Yan Y, Blackburn SL, McBride DW (2019) Neurobehavioral Deficits After Subarachnoid Hemorrhage in Mice: Sensitivity Analysis and Development of a New Composite Score. *J Am Heart Assoc* 8 (8): e011699. doi: 10.1161/jaha.118.011699
- Koźba-Goszyła M, Czapiga B, Jarmundowicz W (2015) Aneurismal subarachnoid hemorrhage: who remains for surgical treatment in the post-ISAT era? *Archives of medical science : AMS* 11 (3): 536-543. doi: 10.5114/aoms.2013.37333
- Neifert SN, Chapman EK, Martini ML, Shuman WH, Schupper AJ, Oermann EK, Mocco J, Macdonald RL (2021) Aneurysmal

- Subarachnoid Hemorrhage: the Last Decade. *Transl Stroke Res* 12 (3): 428-446. doi: 10.1007/s12975-020-00867-0
17. Acuña MY, L AC (2011) Aneurysmal subarachnoid hemorrhage in a Chilean population, with emphasis on risk factors. *BMC Res Notes* 4: 464. doi: 10.1186/1756-0500-4-464
 18. Zhang P, Li Y, Zhang H, Wang X, Dong L, Yan Z, She L, Wang X, Wei M, Tang C (2023) Prognostic value of the systemic inflammation response index in patients with aneurysmal subarachnoid hemorrhage and a Nomogram model construction. *Br J Neurosurg* 37 (6): 1560-1566. doi: 10.1080/02688697.2020.1831438
 19. Hawryluk GWJ, Citerio G, Hutchinson P, Koliás A, Meyfroidt G, Robba C, Stocchetti N, Chesnut R (2022) Intracranial pressure: current perspectives on physiology and monitoring. *Intensive Care Med* 48 (10): 1471-1481. doi: 10.1007/s00134-022-06786-y
 20. Feiler S, Friedrich B, Schöller K, Thal SC, Plesnila N (2010) Standardized induction of subarachnoid hemorrhage in mice by intracranial pressure monitoring. *J Neurosci Methods* 190 (2): 164-170. doi: 10.1016/j.jneumeth.2010.05.005
 21. Zoerle T, Lombardo A, Colombo A, Longhi L, Zanier ER, Rampini P, Stocchetti N (2015) Intracranial pressure after subarachnoid hemorrhage. *Crit Care Med* 43 (1): 168-176. doi: 10.1097/ccm.0000000000000670
 22. Olson DM, Zomorodi M, Britz GW, Zomorodi AR, Amato A, Graffagnino C (2013) Continuous cerebral spinal fluid drainage associated with complications in patients admitted with subarachnoid hemorrhage. *J Neurosurg* 119 (4): 974-980. doi: 10.3171/2013.6.Jns122403
 23. Burzyńska M, Uryga A, Załuski R, Goździk A, Adamik B, Robba C, Goździk W (2023) Cerebrospinal Fluid and Serum Biomarker Insights in Aneurysmal Subarachnoid Haemorrhage: Navigating the Brain-Heart Interrelationship for Improved Patient Outcomes. *Biomedicines* 11 (10). doi: 10.3390/biomedicines11102835
 24. Sanchez-Peña P, Pereira AR, Sourour NA, Biondi A, Lejean L, Colonne C, Boch AL, Al Hawari M, Abdenour L, Puybasset L (2008) S100B as an additional prognostic marker in subarachnoid aneurysmal hemorrhage. *Crit Care Med* 36 (8): 2267-2273. doi: 10.1097/CCM.0b013e3181809750
 25. Pulcrano-Nicolas AS, Proust C, Clarençon F, Jacquens A, Perret C, Roux M, Shotar E, Thibord F, Puybasset L, Garnier S, Degos V, Trégouët DA (2018) Whole-Blood miRNA Sequencing Profiling for Vasospasm in Patients With Aneurysmal Subarachnoid Hemorrhage. *Stroke* 49 (9): 2220-2223. doi: 10.1161/strokeaha.118.021101
 26. Zhuang J, Shen L, Li M, Sun J, Hao J, Li J, Zhu Z, Ge S, Zhang D, Guo H, Huang R, Yan J (2023) Cancer-Associated Fibroblast-Derived miR-146a-5p Generates a Niche That Promotes Bladder Cancer Stemness and Chemoresistance. *Cancer Res* 83 (10): 1611-1627. doi: 10.1158/0008-5472.Can-22-2213
 27. Lu Y, Cao DL, Jiang BC, Yang T, Gao YJ (2015) MicroRNA-146a-5p attenuates neuropathic pain via suppressing TRAF6 signaling in the spinal cord. *Brain Behav Immun* 49: 119-129. doi: 10.1016/j.bbi.2015.04.018
 28. Al-Mufti F, Amuluru K, Smith B, Damodara N, El-Ghanem M, Singh IP, Dangayach N, Gandhi CD (2017) Emerging Markers of Early Brain Injury and Delayed Cerebral Ischemia in Aneurysmal Subarachnoid Hemorrhage. *World Neurosurg* 107: 148-159. doi: 10.1016/j.wneu.2017.07.114
 29. Fan H, Ding R, Liu W, Zhang X, Li R, Wei B, Su S, Jin F, Wei C, He X, Li X, Duan C (2021) Heat shock protein 22 modulates NRF1/TFAM-dependent mitochondrial biogenesis and DRP1-sparked mitochondrial apoptosis through AMPK-PGC1 α signaling pathway to alleviate the early brain injury of subarachnoid hemorrhage in rats. *Redox Biol* 40: 101856. doi: 10.1016/j.redox.2021.101856
 30. Shao J, Meng Y, Yuan K, Wu Q, Zhu S, Li Y, Wu P, Zheng J, Shi H (2023) RU.521 mitigates subarachnoid hemorrhage-induced brain injury via regulating microglial polarization and neuroinflammation mediated by the cGAS/STING/NF- κ B pathway. *Cell Commun Signal* 21 (1): 264. doi: 10.1186/s12964-023-01274-2
 31. Mai H, Fan W, Wang Y, Cai Y, Li X, Chen F, Chen X, Yang J, Tang P, Chen H, Zou T, Hong T, Wan C, Zhao B, Cui L (2019) Intranasal Administration of miR-146a Agomir Rescued the Pathological Process and Cognitive Impairment in an AD Mouse Model. *Mol Ther Nucleic Acids* 18: 681-695. doi: 10.1016/j.omtn.2019.10.002
 32. Lin H, Kryczek I, Li S, Green MD, Ali A, Hamasha R, Wei S, Vatan L, Szeliga W, Grove S, Li X, Li J, Wang W, Yan Y, Choi JE, Li G, Bian Y, Xu Y, Zhou J, Yu J, Xia H, Wang W, Alva A, Chinnaiyan AM, Cieslik M, Zou W (2021) Stanniocalcin 1 is a phagocytosis checkpoint driving tumor immune resistance. *Cancer Cell* 39 (4): 480-493.e486. doi: 10.1016/j.ccell.2020.12.023
 33. Luo M, Wang X, Wu S, Yang C, Su Q, Huang L, Fu K, An S, Xie F, To KKW, Wang F, Fu L (2023) A20 promotes colorectal cancer immune evasion by upregulating STC1 expression to block "eat-me" signal. *Signal Transduct Target Ther* 8 (1): 312. doi: 10.1038/s41392-023-01545-x
 34. Li Y, He ZC, Zhang XN, Liu Q, Chen C, Zhu Z, Chen Q, Shi Y, Yao XH, Cui YH, Zhang X, Wang Y, Kung HF, Ping YF, Bian XW (2018) Stanniocalcin-1 augments stem-like traits of glioblastoma cells through binding and activating NOTCH1. *Cancer Lett* 416: 66-74. doi: 10.1016/j.canlet.2017.11.033
 35. Zarei H, Nemati S (2024) Evaluation of prebiotic supplementation on lipid peroxidation and hematologic parameters of broilers with ascites. *J Poult Sci Avian Dis* 2(2): 1-7. <https://jpsad.com/index.php/jpsad/article/view/39>
 36. Mansoor, S, Ullah I, Khan N (2024) Diversity and antibiotic resistance profile analysis of uropathogenic bacteria in human and canines. *Cell Mol Biomed Rep* 4(2): 65-73. doi: 10.55705/cnbr.2023.411879.1169
 37. Jun Q, Luo W (2021) Early-stage serum Stanniocalcin 1 as a predictor of outcome in patients with aneurysmal subarachnoid hemorrhage. *Medicine (Baltimore)* 100 (51): e28222. doi: 10.1097/md.0000000000002822